



COLLOCATED STRUCTURAL CONTROL FOR REDUCTION OF AIRCRAFT CABIN NOISE

DOUGLAS G. MACMARTIN

United Technologies Research Center, East Hartford, Connecticut, 06108, U.S.A.

(Received 28 November 1994 and in final form 11 May 1995)

Various approaches to cabin noise reduction within turbo-prop aircraft have been suggested. Since the primary source of internal noise is due to propeller-induced fuselage vibration, the noise can be reduced by minimizing the noise transmission through the fuselage using active structural control. The feasibility of a structural control approach using piezoelectric actuators and structural sensors is investigated. Feedback of collocated strain yields an approach which is simple, modular, and extremely robust. Actuator and sensor selection is based on wave-number arguments. Simulations with a simple vibro-acoustic aircraft model indicate that the desired goal of a 10 dBA reduction in peak internal noise is achievable with relatively few actuators. Various actuator/sensor placement and control architecture configurations are investigated with the eventual goal of minimizing the total weight penalty.

© 1996 Academic Press Limited

1. INTRODUCTION

There is a desire to reduce the cabin noise within commercial turbo-prop aircraft, in order to improve passenger comfort [1]. The cabin noise is generated by various sources, including boundary layer flow noise, acoustic excitation of the fuselage from the propeller, and structure-borne noise due to engine vibration and flow distortion over the wing. For typical turbo-prop aircraft, the proximity of the propeller disc to the fuselage results in the narrow-band acoustic excitation of the fuselage being the dominant source of noise. The objective is to reduce the peak interior noise level by approximately 10 dBA.

Noise reduction options include both passive methods, such as structural modifications [2] or damping augmentation [3, 4], and active methods, including synchrophasing, and control of either the acoustic field [5, 6] or the structural vibration [7–10]. Stiffening the structure tends to incur a substantial weight penalty. Broadband passive damping is not useful because the response is primarily forced, rather than resonant. Narrowband damping using tuned vibration absorbers has yielded 10 dB reductions [3], but the improvement is limited by the difficulty of keeping them tuned in a varying environment. An active approach, however, can be tuned to allow for varying engine speed or environment, and can handle several frequencies simultaneously. There have already been flight tests using active control of the internal sound field which have obtained 10 dB reductions [5, 6]. However, many microphones and speakers are required to obtain this performance, yielding a moderate weight penalty, and some difficulty in locating bulky speakers within the passenger compartment.

An alternative active approach is to eliminate the problem before the sound gets into the aircraft cabin by using active structural control to modify the acoustic transmission properties of the fuselage. This approach has an advantage over directly controlling the

interior noise, in that fewer actuators and sensors are required, since they are only needed near the propeller plane [11, 12]. The concept of controlling structural vibration to reduce transmitted or radiated noise is not new [13], and has been investigated by a variety of researchers for the aircraft noise control problem [7–12]. However, most of the literature on this subject uses sound pressure information from within the cabin. By making the control objective the reduction of noise transmission, rather than of internal noise, an approach can be developed that uses only feedback of local structural information. High gain feedback then reduces fuselage vibration in the propeller footprint area, which reduces the power input from the propeller disturbance, and sound radiation into the aircraft cabin.

Piezoelectric actuators are well suited to this problem due to their low weight, high bandwidth, and because their area-averaging effect reduces their influence on structural modes that do not couple with the acoustic response. In the context of the wave-number based radiative efficiency arguments of reference [14], the distributed piezoelectric actuator and collocated strain sensor act as spatial filters. Fuller *et al.* [10] have used piezoelectric actuators bonded to an aircraft fuselage and obtained acceptable authority over internal noise using microphone feedback, indicating that the required actuator strength is feasible.

To evaluate the capability of a collocated vibration control approach for reducing internal noise, a vibro-acoustic model is developed. Various researchers have investigated active structural and acoustic control for aircraft using simple cylinder models of the structural vibration [15–17]. In addition, there are numerous more detailed modelling techniques available, including finite element and boundary element methods [18]. Since accurate predictions of absolute noise levels are not required, a simple model is sufficient. The model developed herein treats the fuselage as an orthotropic finite cylinder with equivalent bending stiffnesses to account for the frames and stringers, similar to the model in reference [19]. The stiffening effect of the floor is partially included. The closed-loop structural response is obtained for a computer prediction of the propeller sound pressure field. The interior acoustic response is then computed from the structural vibration. The primary objective is to demonstrate that the desired performance goal of a 10 dBA reduction in peak internal noise can be obtained. In addition, different actuator and sensor configurations and control architectures are evaluated, with the ultimate goal of minimizing the weight penalty.

2. CONCEPTUAL DESIGN

One of the objectives that must be considered in developing an approach intended for eventual production is the ease of implementation of the ultimate design. While difficult to quantify, this includes factors such as ease of production and assembly, the impact on other aspects of the overall system, the handling of inevitable sensor/actuator failures, and substantial robustness to the wide range of operating conditions likely to be encountered on numerous different aircraft. Finally, the total system cost and weight must be minimized. With these design objectives in mind, the overall simplicity and modularity of the approach can be as important as the performance it achieves.

One drawback to the use of speakers in the aircraft cabin for noise control is locating them so as to preserve their effect, while protecting them from damage and minimizing any loss in useful space. Prior work on active structural-acoustic control has indicated that structural actuators can be used, rather than speakers. A purely structural control approach that eliminates the needs for microphones can have considerable advantages with regards to the overall design objectives, as described below. The key requirement is to identify an appropriate structural sensor.

Substantial simplifications result by defining the objective to be reducing the noise transmission through the fuselage, rather than reducing the internal noise. These objectives are equivalent in the sense that reducing the former will reduce the latter. However, the internal noise is a global performance objective, while noise transmission depends only on the local structural information at an actuator location. Thus it is sufficient to use collocated feedback, and minimize the sensor output, as indicated schematically in Figure 1. This yields a simple control design problem, and gives substantial robustness. While the transfer function from a piezoelectric actuator to a microphone varies considerably with changes in passenger load and operating conditions, the fundamental characteristics of the local structural transfer functions remain unchanged. This is particularly true if collocated strain sensors are used, since the resulting transfer functions will be positive real. Positive real feedback can then be used to guarantee stability.

This approach is similar to the concept of disturbance isolation, wherein the disturbance is prevented from entering the structure by high gain collocated feedback. This class of solution techniques has typically achieved excellent performance, due in part to the fact that the uncertain dynamics of the structure do not need to be accurately modelled. The control system alters the mode shapes of the system so that the impedance seen by the disturbance is increased. Performance can also be achieved by altering mode shapes to reduce structural-acoustic coupling; this is analogous to performance isolation.

The limitation observed in the literature on purely structural control approaches to noise reduction is that only low wave-number structural motion couples well with the acoustic field [14, 9, 16]. Thus, minimizing structural motion may increase the acoustic response unless the sensors and actuators do not respond to or excite that motion that does not couple well. Choosing the sensor and actuator dimensions on the order of one half of the acoustic wavelength at the frequency of interest results in spatial wave-number filtering. Minimizing the sensor is therefore an approximation to minimizing the acoustic radiation. Precisely sensing the structural motion that radiates efficiently would improve performance, but is neither essential, nor simple.

The piezoelectric actuators will be bonded to the inner surface of the fuselage frames, to give the largest possible moment arm to excite fuselage ring bending. It is the frames which dominate the structural dynamics at the frequencies of interest. If the frames are controlled, then the fuselage skin can still vibrate between the frames. However, on the deHavilland Dash-8, the distance between frames is such that this remaining skin vibration can only couple well with the acoustic field above approximately 300 Hz.

Because the disturbance source is not at a single point, actuators will be required at several circumferential locations on several frames. This leads to several options for the

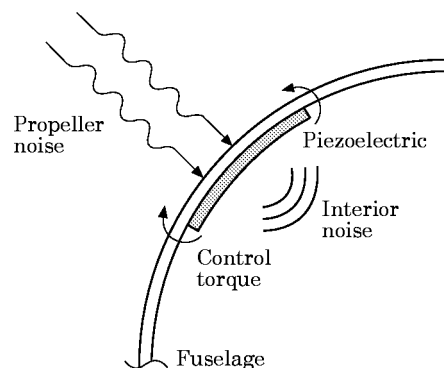


Figure 1. Piezoelectric actuator placement on fuselage frame.

control architecture. A purely decentralized control scheme wherein each actuator uses only single-input/single-output (SISO) feedback of collocated information has numerous advantages. This system would be totally modular, resulting in low computing requirements and associated weight penalty, no redesigns necessary to add additional sensor/actuator pairs, and a very graceful performance degradation to single point failures. These factors can potentially lead to reduced product cost, and reduced installation and maintenance costs, over other approaches.

Each SISO control loop can be tuned to give excellent performance using tachometer information from the engines. Each sensor/actuator pair will effectively behave as a distributed tuned vibration absorber, that is always perfectly tuned with the disturbance frequency, cancels vibrations at the fundamental frequency and desired harmonics, and concentrates its effort on the structural modes that couple efficiently with the acoustics.

Replacing the structural information with microphone feedback would be guaranteed to give better nominal performance, since the true quantity of interest would then be minimized. However, the resulting compensator would have to be both MIMO, and adaptive, which gives increased computational cost, and introduces robustness and fault tolerance issues. Since the noise is caused by structural vibration, clever vibration control can replace microphone feedback. The advantages are simplicity, and potentially lower life-cycle cost.

The distributed collocated structural control architecture is validated analytically herein. The internal noise must be reduced at the propeller blade passage frequency (BPF) and the next few harmonics. The narrowband control for each of these frequencies is completely independent. The control of the fundamental will require the most actuation, since at higher harmonics, the propeller sound pressure distribution on the aircraft is more compact. As a result, the predictions will concentrate on control at the blade passage frequency. The properties of a deHavilland Dash-8 Series 100 fuselage are used for the model, and a predicted propeller sound pressure field corresponding to the Dash-8 is used as the forcing function.

3. VIBRO-ACOUSTIC MODEL DEVELOPMENT

The model must include those features of the real problem that will substantially affect the noise reductions that will be achievable by structural control, however, it need not accurately model the absolute noise levels inside the aircraft. A relatively simple model is therefore sufficient.

The fuselage is modelled as a cylinder with uniform mass and stiffness properties. The bending stiffnesses are calculated from those of the frames and stringers, with the effect of the skin included using shear lag arguments. The primary limitation of this model is that the dynamics are assumed to be dominated by the bending vibrations of the fuselage, and the in-plane extensional vibration is assumed to be much stiffer. As a result of this assumption, ring “breathing” modes are not included, and the lowest bending modes are insufficiently stiff. The effective mass per unit surface area in the model was decreased to match modal frequencies with data from deHavilland. Other simplifying assumptions include:

- (1) Ring and axial bending coupling is not included.
- (2) Deviations of the real fuselage from a cylinder, such as the presence of wings, cockpit, tail, variation in radius of curvature, doors, etc. are not modelled.

- (3) Since the floor adds significant stiffnesses to the structure in a region that would otherwise be strongly affected by the propeller field, this symmetric stiffening effect must be included. All other effects on the floor are ignored.
- (4) All structural and acoustic modes are assumed to have 10% modal damping.
- (5) The passive stiffness of the piezoelectric actuators is not included.
- (6) The acoustic space is modelled as a pure closed cylinder (with no floor).
- (7) The acoustic field does not affect the structural modes.

Polar co-ordinate axes will be used, with r being radial, y longitudinal (axial) and θ circumferential, as shown in Figure 2.

3.1. STRUCTURAL MODEL

The cylinder modes have independent variation in the y and θ directions, indexed separately by i and j . The symmetric $(\cdot)_s$ and anti-symmetric $(\cdot)_a$ mode shapes are [20]

$$\begin{pmatrix} \tilde{r} \\ \tilde{\theta} \end{pmatrix}_s = \begin{pmatrix} i \cos i\theta \cos j\pi y/\ell \\ \sin i\theta \cos j\pi y/\ell \end{pmatrix}, \quad \begin{pmatrix} \tilde{r} \\ \tilde{\theta} \end{pmatrix}_a = \begin{pmatrix} i \sin i\theta \cos j\pi y/\ell \\ -\cos i\theta \cos j\pi y/\ell \end{pmatrix}, \quad (1)$$

where \tilde{r} and $\tilde{\theta}$ are the deflections in the radial and circumferential directions, respectively. The mode $i=1$ involves no frame deformation. The pure extensional mode of each frame, $i=0$, is not included. The modal mass is $m_{ij} = \frac{1}{2} \rho_s \ell R \pi (i^2 + 1)$, the modal stiffness is

$$k_{ij} = i^2 \pi \frac{\ell}{2} \left(\frac{(EI)_y}{d_f R^3} (i^2 - 1)^2 + \frac{R(EI)_z}{d_s} \left(\frac{j\pi}{\ell} \right)^4 \right) \quad (2)$$

and the frequencies are $\omega_{ij} = \sqrt{k_{ij}/m_{ij}}$. The parameters $(EI)_y/d_f$ and $(EI)_z/d_s$ are the average bending stiffnesses per unit length. For small j , the frequencies are dominated by the ring bending stiffness.

The most important difference between the actual fuselage and a pure cylinder model is the stiffening effect of the floor on the symmetric modes. All other effects of the floor are ignored. The additional stiffness between symmetric modes with circumferential mode numbers m and n is $(\Delta K)_{mn} = k_f \phi_m^f \phi_n^f$, where ϕ_m^f is the relative horizontal displacement between the floor attachment points for mode m , given by

$$\phi_m^f = 2(m \cos m\theta_f \sin \theta_f - \sin m\theta_f \cos \theta_f). \quad (3)$$

The effective floor stiffness k_f is chosen to be large with respect to the ring bending stiffness.

The magnitude of the computer predicted propeller sound pressure field at BPF on the port side is shown in Figure 3. Note that, while only the magnitude is shown, the phase

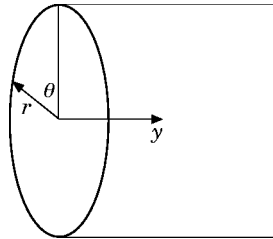


Figure 2. Coordinate axes for model; r is radial, y is longitudinal, and θ is circumferential.

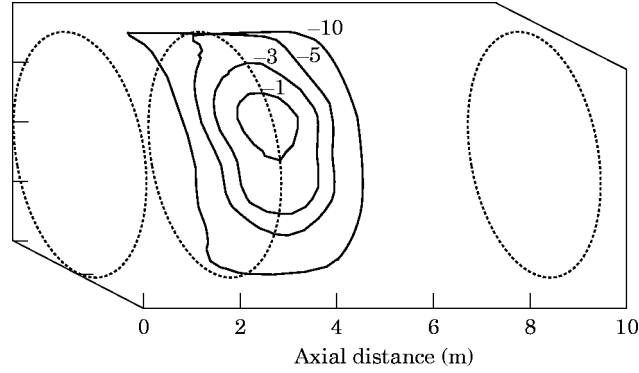


Figure 3. Port side propeller sound pressure magnitude distribution, dB with respect to maximum value. The fore and aft limits of the fuselage and the propeller plane are indicated.

variation is also important when performing the summation over modes. The effect of the disturbance sound pressure is computed as a double integral over θ and y :

$$b_{wij} = \int_0^{\ell} \int_0^{2\pi} P_{ext}(\theta, y) \phi_{ij}(\theta, y) R \, d\theta \, dy, \quad (4)$$

where P_{ext} is the external sound pressure distribution, and ϕ_{ij} the radial displacement of the ij th mode shape.

The free response of a piezoelectric to an applied voltage V is given by the induced strain $A = (d_{31}/d_p)V$. The effect of a piezoelectric actuator bonded to a beam can be approximated by assuming uniform shear within the beam, and constant strain in the piezoelectric [21]. This gives a resulting strain in the beam of

$$\epsilon = \frac{1}{1 + \psi_b} A, \quad \text{where} \quad \psi_b = \frac{(EI)_s}{t^2(EA)_p}. \quad (5)$$

A finite length piezoelectric is typically modelled as applying pin forces F at the ends of the actuator, where

$$F = (EA)_p \frac{\psi_b}{1 + \psi_b} A = \mu V. \quad (6)$$

For actuators bonded to the inner surface of the fuselage frames, this force affects each mode through the circumferential displacement $\tilde{\theta}$, as well as applying a moment. For the fuselage parameters considered here, the force effect of the piezo is larger than the moment effect for $i < 4$.

The pin force model is reasonable when the actuator length is small compared to the wavelengths of the modes of interest. However, this is a poor assumption to use for this model, since one of the advantages in using piezoelectric actuators is that their area-averaging effect reduces their authority over high wavenumber modes that do not couple effectively to the interior acoustic field. Instead, the piezo effectiveness on each mode is computed by integrating over the linearly varying shear force distribution generated by the actuator. For a piezoelectric actuator that runs from a circumferential

angle of $\underline{\theta}$ to $\bar{\theta}$, define $\theta_c = (\bar{\theta} + \underline{\theta})/2$ and $\Delta\theta = (\bar{\theta} - \underline{\theta})/2$. Then the shear stress as a function of θ and the equivalent pin force F is

$$S = \frac{2F}{R\Delta\theta} \frac{(\theta - \theta_c)}{\Delta\theta}. \quad (7)$$

Evaluating the resulting integral yields the piezoelectric effectiveness per volt as

$$b_{p_i}^s = \frac{2}{\mu} \left(1 + \frac{t}{R} i^2\right) \left(\frac{(\sin i\bar{\theta} - \sin i\underline{\theta})}{(i\Delta\theta)^2} - \frac{(\cos i\bar{\theta} + \cos i\underline{\theta})}{i\Delta\theta} \right) \cos \frac{j\pi y}{\ell} \quad (8)$$

for the symmetric modes, with a corresponding expression for the anti-symmetric modes. For $\Delta\theta \rightarrow 0$, equation (8) is equivalent to assuming pin forces applied at the weighted centre of the shear force distribution. The modal response of the collocated strain sensors is the same as the modal influence of the piezoelectric actuators.

The structural model ultimately yields the amplitudes q^s and q^a of the assumed symmetric and anti-symmetric mode shapes, from which the surface velocity of the fuselage can be predicted by summation. In addition to computing the resulting acoustic response, it is useful to compute the power input to the structure by the propeller disturbance, and the total vibrational energy in the structure, given by

$$\Pi_{in} = \omega_0 \sum_i \sum_j i(b_{w_{ij}}^s q_{ij}^s + b_{w_{ij}}^a q_{ij}^a), \quad (9)$$

$$E_s = \sum_i \sum_j (M_{ij} \omega_0^2 + K_{ij}) ((q_{ij}^s)^2 + (q_{ij}^a)^2). \quad (10)$$

The power input at a point, $\Pi_{in}(\theta, y)$, can be computed from the surface velocity and the propeller disturbance, and is useful for determining potential actuator locations. The open-loop contribution of different modes to the total energy, shown in Figure 4, indicates that circumferential modes $i > 5$ and axial modes $j > 13$ do not contribute substantially, and can be eliminated from the model. Modes $i = 3, j \leq 9$ dominate, due to a good match with the disturbance in both frequency and mode shape. At higher harmonics, many more

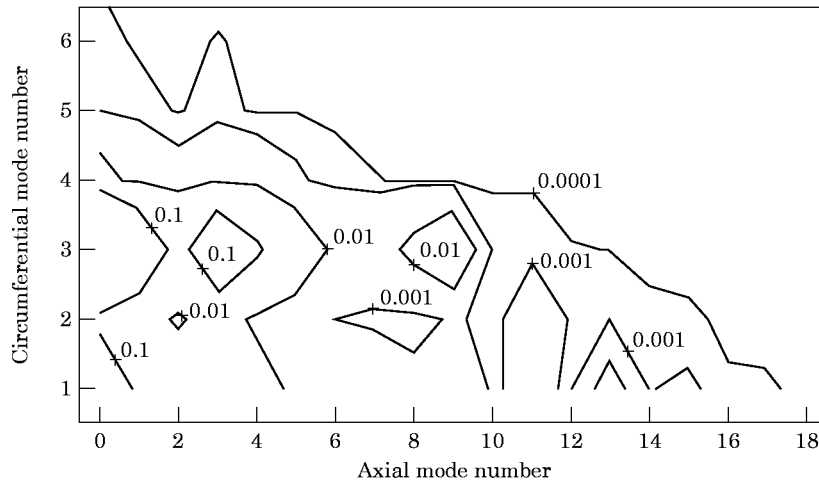


Figure 4. Contribution to total energy by mode number at the blade passage frequency. Contributions from symmetric and anti-symmetric modes are grouped together.

modes contribute, due to both the higher frequency of the disturbance, and to the higher spatial wavenumber content of the disturbance. As a result, it is more difficult to get an accurate characterization of the response.

3.2. ACOUSTIC RESPONSE

The mode shapes for the sound pressure in a cylinder are indexed by i , j , and k ; corresponding to variations in the circumferential, axial, and radial directions, respectively. The symmetric mode shapes are [20]:

$$\psi_{ijk}^s(\theta, y, r) = J_i(\lambda_{ik} r/R) \cos(j\pi y/\ell) \cos i\theta, \quad i, j, k = 0, 1, \dots, \quad (11)$$

with frequency $\omega_{ijk} = c\sqrt{\lambda_{ik}^2/R^2 + j^2\pi^2/\ell^2}$, where J_i is a Bessel function, and λ_{ik} satisfies $J_i'(\lambda_{ik}) = 0$. The anti-symmetric modes have identical frequencies, and circumferential variation $\sin i\theta$ rather than $\cos i\theta$.

From Nelson and Elliot [22] the total sound pressure is given by

$$P(\theta, y, r) = -\omega_0 \rho c^2 \sum_{i,j,k} \left(\frac{f_{ijk} \psi_{ijk}(\theta, y, r)}{V_{ijk} (-\omega_0^2 + 2\zeta_a \omega_{ijk} \omega_0 + \omega_{ijk}^2)} \right). \quad (12)$$

The summation includes both the symmetric and anti-symmetric modes. The modal volume V_{ijk} is the integral of ψ_{ijk}^2 over the internal volume, and ζ_a is the assumed damping ratio of the acoustic modes. The quantity f_{ijk} is the generalized force on mode (i, j, k) , given by the integral over the fuselage surface area of the mode shape $\psi_{ijk}(\theta, y, 1)$ multiplied by the surface velocity predicted by the structural model. By orthogonality, the acoustic mode ψ_{ijk}^s couples only with the structural mode ϕ_{ij}^s , and ψ_{ijk}^a couples only with ϕ_{ij}^a . The generalized forces in equation (12) are given by

$$f_{ijk} = q_{ij} \frac{iR\pi\ell\omega_0}{2} J_i(\lambda_{ik}), \quad (13)$$

with q_{ij}^s being used for symmetric acoustic modes, and q_{ij}^a for antisymmetric ones. Note that the $i=0$ acoustic modes do not couple with any of the assumed structural modes; this corresponds to a pure breathing mode of the ring which does not involve any bending motion.

The goal is to minimize the peak internal sound pressure. An alternative performance measure is the total acoustic potential energy, given by

$$E_{ac} = \sum_{i,j,k} \frac{V_{ijk}}{4\rho c^2} ((q_{ijk}^s)^2 + (q_{ijk}^a)^2), \quad (14)$$

where q_{ijk} are the amplitudes of the acoustic modes, given by the terms in brackets in equation (12).

One of the key assumptions made in the conceptual design of the control architecture was that only the low wave-number structural modes couple well with the acoustic response. While this is true for an infinite flat plate radiating into a half-space [14], the coupling is more complicated for an enclosed cylinder, and there is no cut-off phenomenon wherein certain modes do not couple at all. The structural-acoustic coupling predicted by this model is plotted in Figure 5. The coupling is computed per structural mode, and plotted as a function of wave number. Also shown is the cut-off wave-number predicted by infinite flat plate theory, and the wave-number filtering provided by the distributed actuator and sensor.

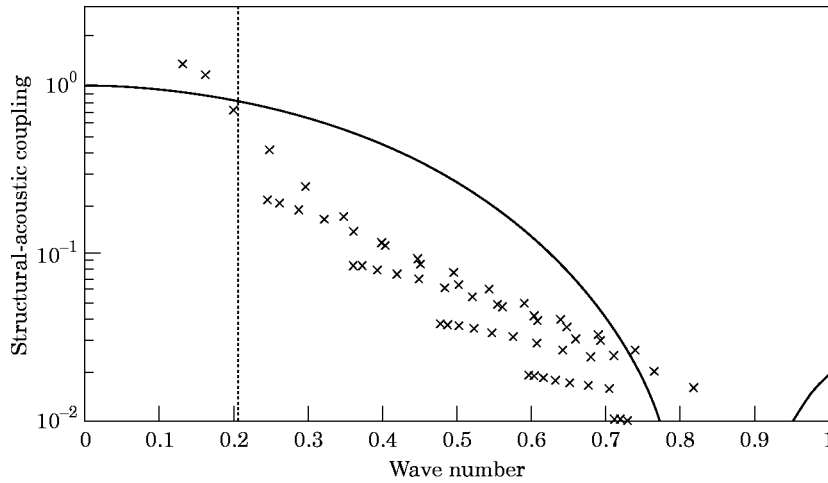


Figure 5. Structural-acoustic coupling as a function of wave-number: \times predicted by model; \cdots cut-off wave number predicted by infinite flat plate theory; — wave-number filtering provided by the distributed sensor and actuator.

3.3. MODEL VALIDATION

A deHavilland Dash-8 Series 100 fuselage was available for testing. This fuselage was used in previous studies of propeller noise transmission [23]. Although a complete modal analysis of the fuselage was not performed, the predicted circumferential bending frequencies are within about 10% of the measured values for the modes near the blade passage frequency. Because of the high acoustic modal density on both the model and the aircraft in the frequency range of interest, it is difficult to compare acoustic mode frequencies and shapes.

The turbo-prop noise control application demands that the piezoelectrics be capable of generating substantial strains in the fuselage frames. The maximum strain that can be induced in the structure is related to the relative stiffness of the piezoelectric actuator and the structure, given by the parameter ψ_b in equation (5). Therefore, a relatively thick crystal that is approximately impedance matched to the structure is desired. For implementation, a layered actuator can be used to reduce voltage requirements.

In order to verify the strain that could be induced, several actuators were bonded to the fuselage, and the resulting strain measured. The predicted levels were achieved, indicating that equation (5) is approximately valid, even though flat actuators were bonded to a curved surface. Estimates of the in-flight dynamic strain that the piezoelectric actuators will encounter are lower than the maximum capability indicated by the preliminary experimentation.

4. CONTROL DESIGN

There are several approaches that could be used to design control systems for this problem. Much of the work on noise control has used an LMS adaptive disturbance feedforward algorithm, while much of the research in the related area of vibration control has used standard feedback design techniques. It can be shown, however, that for harmonic disturbances, the two approaches yield identical controllers [24], and therefore for analysis purposes, linear feedback was used. Controllers were designed using low order, classical

frequency domain techniques, and applied to the state space model of the fuselage to obtain the closed loop modal amplitudes.

The simplest control architecture is to design independent controllers for each sensor/actuator pair. High gain is desired at the disturbance frequency, ω_0 , in order to minimize the average strain over the region covered by each actuator. The transfer function for each compensator is of the form

$$K_i(s) = \frac{2\alpha\omega_0}{|G(j\omega_0)|} \left(\frac{s}{s^2 + 2\zeta_c\omega_0s + \omega_0^2} \right), \quad (15)$$

where $G(j\omega_0)$ is the transfer function from an actuator to the collocated sensor, evaluated at the excitation frequency ω_0 , and α is a gain parameter. This lightly damped second order system is a standard compensator for tonal control, and can be easily implemented with a slowly time-varying excitation frequency ω_0 [25]. Stability-robustness is guaranteed because both the compensator and the plant are positive real. Performance is obtained with high gain at the disturbance frequency; the sensor output is reduced by a factor of α/ζ_c . Increasing α increases the gain at frequencies away from the disturbance, which may increase broadband noise problems. Decreasing ζ_c makes the frequency range of disturbance attenuation narrower, which is acceptable if the disturbance frequency is constant. For the simulations, the compensator design parameters were selected to reduce the sensor output to 1% of its former value. Further reductions will not yield substantial further improvements in the acoustic response, since this will now be dominated by the fuselage response elsewhere.

5. PREDICTIONS FROM MODEL

The structural modelling and sound pressure distribution information can be used to predict the surface vibrational velocity distribution, and the corresponding distribution of input power at the blade passage frequency. The predicted input power is shown in Figure 6, with the starboard side of the aircraft on the left, and the front of the cabin at the bottom. The bottom of the fuselage is in the centre of the plot, and the top at the edges.

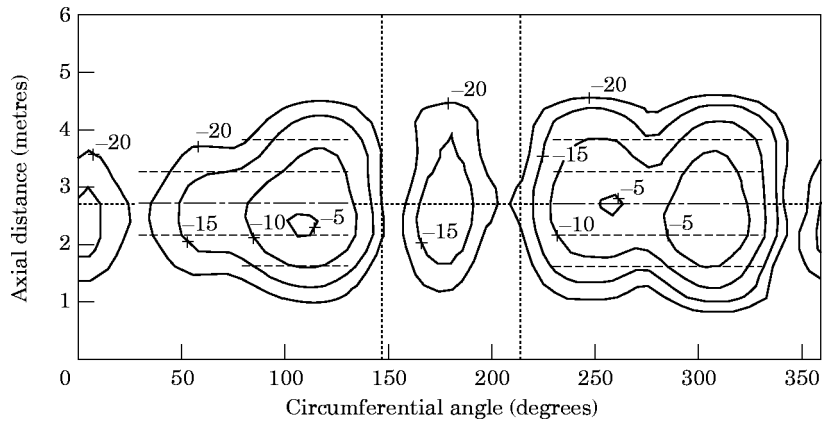


Figure 6. Predicted open-loop input power distribution, in dB with respect to the peak input power. A potential set of actuator locations is shown with dashed lines. The axial location of the propeller plane, and circumferential angle of the floor locations are indicated with dotted lines.

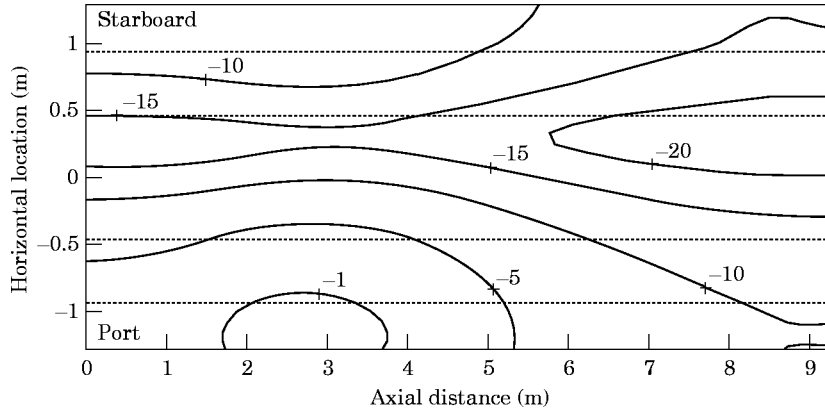


Figure 7. Predicted open-loop internal acoustic response at passenger head height, dB with respect to peak. The axial location of the propeller plane, and the horizontal location of passenger seats are shown with dotted lines.

The purpose in plotting the input power distribution is to determine good actuator locations, and a potential set is shown in this figure.

The predicted open-loop internal acoustic field is shown in Figure 7. The peak response is on the port side of the aircraft, near the propeller plane. The actuator locations indicated in Figure 6 were then used to obtain the closed-loop acoustic field in Figure 8. This configuration meets the performance goal of a 10 dB reduction in peak internal noise, indicating that this goal is feasible. Independent control laws were used for all actuator/sensor pairs, and all actuators covered a 50° arc of a single frame. The total weight of piezoelectrics in this configuration is approximately 16 kg. The weight penalty could be reduced with additional optimization of the control architecture, actuator locations, and the actuators themselves.

Neither the total input power, nor the total vibrational energy within the structure are representative of the peak internal noise, as was noted by Thomas *et al.* [16]. This is due to the fact that not all structural modes couple equally well with the acoustic field, and thus the energy in some modes is not as important as the energy in others. This result is evident in Figure 9, which gives both the open-loop and closed-loop energy in the structure

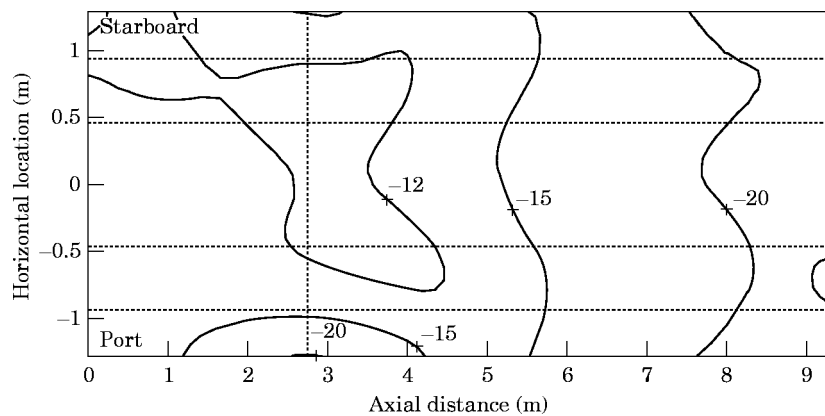


Figure 8. Predicted closed-loop internal acoustic response at passenger head height, dB with respect to open-loop peak, using 18 actuators. The axial location of the propeller plane, and the horizontal location of passenger seats are shown with dotted lines.

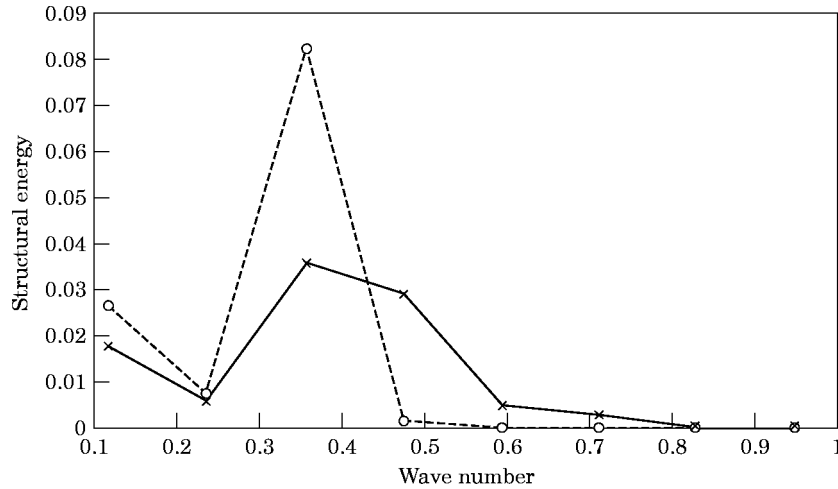


Figure 9. Structural energy as a function of circumferential wave-number; ---- open-loop, — closed-loop.

as a function of circumferential wave-number. While the total structural energy has been decreased only slightly, some energy has been shifted from low wave-number modes which couple well with the acoustic field, to higher wave-number modes where the energy has little effect (see Figure 5). This result is particularly important, as it indicates how the control approach results in the achieved noise reduction. Also note that while the total structural vibrational energy is a poor measure of the acoustic performance, structural vibration is also a problem, and therefore it is necessary to monitor the structural energy to ensure that it does not increase substantially.

Closed-loop results for various actuator configurations are summarized in Table 1, which lists the power input to the structure, the structural energy, the acoustic potential energy, and the peak internal noise. The cases with 1 and 3 actuators have all of the actuators near the peak of the sound pressure disturbance on the port side, the next case has actuators on both sides of the aircraft. These show the gradual improvement with additional actuators, however, none of them has sufficient actuators to prevent sound from entering the cabin. An inadvertent variation in the modal damping between symmetric and asymmetric modes is responsible for the occasional slight increase in total structural energy observed, even though the total input power is reduced, and the compensator is purely dissipative.

TABLE 1

Input power, structural vibrational energy, acoustic potential energy, and reduction in peak internal cabin noise for various actuator and sensor locations, and configurations; all dB with respect to open-loop

Case	# Actuators	Π_{in} (dB)	E_s (dB)	E_{ac} (dB)	P_{max} (dB)
—	0	0	0	0	0
1	1	-0.38	0.56	0.10	-0.55
2	3	-1.33	-0.22	-0.29	-2.09
3	9	-2.92	2.09	-2.32	-4.95
4	18	-2.90	-0.81	-3.56	-11.21
5	18/4	-0.71	0.21	-3.28	-9.88
6	12/2	-1.05	0.22	-3.07	-8.78

Case 4 corresponds to the actuator locations in Figure 8. This is the minimum coverage required for this model to obtain sufficient noise reductions. Optimizing the placement is important, as different configurations with the same number of actuators can yield significantly different performance. While a complete numerical optimization was not performed, the locations were chosen to cover the peak areas of the input power distribution, so that the specified external disturbance could be cancelled.

In addition to optimizing actuator locations, a comparison of alternate control architectures with a given selection can be made. Two additional cases are shown in Table 1. For case 5, the same actuators were grouped together so that only four separate control loops were used. Although some modularity is sacrificed by requiring connections between actuators on adjacent frames, the control hardware is simplified substantially. The additional simplicity is gained with only a 1-4 dB increase in internal noise. The final case indicates that it may not be necessary to actuate in all of the locations indicated in Figure 8. It may be sufficient only to sense the strain in the frames furthest from the propeller plane, and allow actuators to use sensor information from neighbouring frames. In case 6, all the actuators on one side of the aircraft were grouped together. Similar information to the previous two cases was available, but only 12 of the previous 18 actuators were used. The reduction obtained in this case is 1.6 dB better than if only collocated information were available.

Finally, the 18 actuator locations from Figure 6 were used with a different external sound pressure distribution corresponding to a 15% change in engine rpm. In addition to the change in the applied pressure distribution, the structural and acoustic dynamics evaluated at the disturbance frequency also changed, which resulted in different modes being excited. At this second frequency, the results were superior. The control achieved a 13 dB reduction in peak sound pressure, accompanied by significant decrease in input power, structural energy, and acoustic energy. This verifies that the control architecture and actuator locations are robust to variations in both the details of the propeller sound pressure footprint, and in the structural and acoustic dynamics.

6. CONCLUSIONS

There is a desire to reduce the level of cabin noise in turbo-prop aircraft. A promising approach is to use active structural control to minimize the fuselage noise transmission in the vicinity of the propeller noise "footprint". A simple, robust, and modular system can be obtained by placing piezoelectric actuators on the fuselage frames near the propeller plane, and using collocated strain feedback to reduce the noise transmission. Simulations with a simple vibro-acoustic model indicate that the desired goal of a 10 dBA reduction in peak internal noise is feasible with fewer actuators and a lower weight penalty than existing speaker-based active noise control systems. A proper comparison of structural actuators versus speakers, and collocated feedback of structural sensors versus microphone feedback, must be based on the total life-cycle cost of any option for a given performance.

The weight penalty required to achieve the specified performance objective can be minimized by studying different actuator/sensor placements and control architectures. Using feedback of strain information from neighbouring frames in addition to the collocated information was shown to improve performance. The computational burden can be reduced by grouping actuators on different frames together. The simulations indicate that only a few distinct control loops are required.

ACKNOWLEDGMENTS

This work was conducted as part of a collaborative research and development project between deHavilland Inc. and the National Research Council of Canada, while the author was with the Institute for Aerospace Research at NRC. Propeller sound pressure field and structural information were obtained from deHavilland Inc. The assistance of deHavilland, and of the rest of the staff at the Aeroacoustics Facility of NRC is greatly appreciated. Thanks also to Dr. Andreas von Flotow for his comments.

REFERENCES

1. J. S. MIXSON and C. A. POWELL 1984 *AIAA/NASA 9th Aeroacoustics Conference*, (Williamsburg, VA). Review of Recent Research on Interior Noise of Propeller Aircraft. (AIAA Paper 84-2349).
2. R. B. BHAT, J. SOBIESZCZANSKI and J. S. MIXSON 1977 *Noisexpo*, 40–45. Reduction of aircraft cabin noise by fuselage structural optimization.
3. E. H. WATERMAN, D. KAPTEIN and S. L. SARIN 1983 *SAE Paper* 830736. Fokker's activities in cabin noise control for propeller aircraft.
4. W. G. HALVORSEN and U. EMBORG 1989 *SAE Paper* 891080, *General aviation aircraft meeting and exposition*. Interior noise control of the Saab 340 Aircraft.
5. S. J. ELLIOT, P. A. NELSON, I. M. STOTHERS and C. C. BOUCHER 1990 *Journal of Sound and Vibration* **140**, 219–238. In-flight experiments on the active control of propeller-induced cabin noise.
6. I. U. BORCHERS, K. RENGER, J. PAILLARD, G. BILLOUD, P. KOERS and E. DOPPENBERG 1993 *Inter-Noise*, (Leuven, Belgium), 59–64. Selected flight test data and control system results of the CEC BRITE/EURAM ASANCA study.
7. M. A. SIMPSON, T. M. LUONG, C. R. FULLER and J. D. JONES 1991 *AIAA J. Aircraft* **28**, 208–215. Full-scale demonstration tests of cabin noise reduction using active vibration control.
8. C. R. FULLER, S. D. SNYDER, C. H. HANSEN and R. J. SILCOX 1992 *AIAA Journal* **30**, 2613–2617. Active control of interior noise in model aircraft fuselages using piezoceramic actuators.
9. R. J. SILCOX, S. LEFEBVRE, V. L. METCALF, T. B. BEYER and C. R. FULLER 1992 *Proc., DGLR/AIAA 14th Aeroacoustics Conference*, 542–551. Evaluation of piezoceramic actuators for control of aircraft interior noise.
10. C. R. FULLER and G. P. GIBBS 1994 *Noise-Con 94*, (Ft. Lauderdale, Florida). Active control of interior noise in a business jet using piezoceramic actuators.
11. R. J. SILCOX, C. R. FULLER and H. C. LESTER 1990 *AIAA Journal* **28**, 1397–1404. Mechanisms of active control in cylindrical fuselage structures.
12. D. J. ROSSETTI, M. A. NORRIS, S. C. SOUTHWARD and J. Q. SUN 1993 *Recent Advances in Active Control of Sound and Vibration*, (Blacksburg, Virginia), *VPI and SU, Technomic*. A comparison of speakers and structural-based actuators for aircraft cabin noise control.
13. A. I. VYALYSHEV and B. D. TARTAKOVSKII 1976 *Soviet Phys. Acoustics* **22**, 382–385. Radiation compensation of a flexurally vibrating plate at subcritical frequencies.
14. C. R. FULLER and R. A. BURDISO 1991 *Journal of Sound and Vibration* **148**, 355–360. A wavenumber domain approach to the active control of structure-borne sound.
15. A. J. BULLMORE, P. A. NELSON and S. J. ELLIOT 1990 *Journal of Sound and Vibration* **140**, 191–217. Theoretical studies of the active control of propeller-induced cabin noise.
16. D. R. THOMAS, P. A. NELSON and S. J. ELLIOT 1993 *Journal of Sound and Vibration* **167**, 91–111. Active control of the transmission of sound through a thin cylindrical shell, Part I: The minimization of vibrational energy.
17. H. C. LESTER and S. LEFEBVRE 1993 *J. of Intelligent Materials Systems and Structures* **4**, 295–306. Piezoelectric actuator models for active sound and vibration control of cylinders.
18. R. S. LANGLEY 1993 *Journal of Sound and Vibration* **163**, 207–230. A dynamic stiffness/boundary element method for the prediction of interior noise levels.
19. H. C. NELSON, B. ZAPOTOWSKI and M. BERNSTEIN 1958 *Proceedings, National Specialists Meeting on Dynamics and Aeroelasticity* (Fort Worth, Texas) 77–87. Vibration analysis of an orthogonally stiffened circular fuselage and comparison with experiment.
20. R. D. BLEVINS 1979 *Formulas for Frequency and Mode Shape*. Malabar, Florida: Robert Krieger.
21. E. H. ANDERSON 1989 *Master's thesis, Massachusetts Institute of Technology—Space Systems Laboratory Report* 5–89. Induced strain actuation of one- and two-dimensional structures.

22. P. A. NELSON and S. J. ELLIOT 1992 *Active Control of Sound*. London: Academic Press.
23. D. G. MACMARTIN, G. L. BASSO and F. W. SLINGERLAND 1995 *Journal of Sound and Vibration* **187**, 467–483. Aircraft fuselage noise transmission measurements using a reciprocity technique.
24. D. G. MACMARTIN 1994 *American Control Conference (Baltimore, MD)*, 1632–1636. A feedback perspective on the LSM disturbance feedforward algorithm.
25. K. B. SCRIBNER, L. A. SIEVERS and A. H. VON FLOTOW 1993 *Journal of Sound and Vibration* **167**, 17–40. Active narrow-band vibration isolation of machinery noise from resonant substructures.

APPENDIX: NOTATION

ω_0	disturbance frequency	$(EI)_z$	axial bending stiffness per stringer
R	radius of fuselage	$(EA)_p$	extensional stiffness of piezo
ℓ	length of aircraft cabin	d_p	thickness of piezoelectric
d_f	frame spacing	t	distance, piezo to frame neutral axis
d_s	stringer spacing	d_{31}	piezoelectric strain constant
θ_f	floor angle, from top of aircraft	ρ	density of air
ρ_s	effective mass per unit surface area	c	speed of sound in air
$(EI)_y$	ring bending stiffness per frame		